aerospace

MDPI

*Article*

# Heat Shield Properties of Lightweight Ablator Series for Transfer Vehicle Systems with Different Laminated Structures Under High Enthalpy Flow Environments

**Masayuki Ohkage, Kei-ichi Okuyama *, Soichiro Hori and Tsumugi Ishida**

Department of Aerospace Engineering, College of Science and Technology, Nihon University, 7-24-1 Narashinodai, Funabashi 274-8501, Chiba, Japan; csma23003@g.nihon-u.ac.jp (M.O.)
* Correspondence: okuyama.keiichi@nihon-u.ac.jp

**Abstract:** The thermal protection system of a re-entry vehicle requires a high-heat-resistant heat shield to protect the spacecraft. Most of the ablative materials developed so far have high heat resistance but have technical issues such as long production times. In this study, we propose a new ablative material (LATS/PEEK) consisting of PEEK and carbon felt as a material that can solve these problems. PEEK has excellent properties such as a short production time and its ability to be produced using 3D printer technology. In addition, PEEK can be molded with a variety of fusion bonding methods, so it is possible to mold the heat shield and structural components as a single structure. However, heating tests conducted in previous research have confirmed the expansion phenomenon of CF/PEEK produced by 3D printers. The expansion of the ablative material is undesirable because it changes the aerodynamic characteristics during re-entry flight. Therefore, the purpose of this research is to clarify the mechanism of the expansion phenomenon of the ablative material based on PEEK resin. Therefore, we conducted thermal gravimetric analysis (TGA) and thermomechanical analysis (TMA) and concluded that the expansion phenomenon during the heating test was caused by the pressure increase inside the ablative material due to pyrolysis gas. Based on this mechanism, we developed a new 3D LATS/PEEK with a structure that can actively release pyrolysis gas, and we conducted a heating test using an arc-heating wind tunnel. As a result, it was found that 3D LATS/PEEK had less expansion and deformation during the heating test than CF/PEEK manufactured using a 3D printer.

**Keywords:** heat shield system; lightweight ablator; CFRP (carbon fiber-reinforced plastic); CFRTP (carbon fiber-reinforced thermoplastic); PEEK (poly ether ether ketone); re-entry; arc wind tunnel

Academic Editor: Hyun-Ung Oh

Received: 28 February 2025
Revised: 21 March 2025
Accepted: 25 March 2025
Published: 27 March 2025

**Citation:** Ohkage, M.; Okuyama, K.-i.; Hori, S.; Ishida, T. Heat Shield Properties of Lightweight Ablator Series for Transfer Vehicle Systems with Different Laminated Structures Under High Enthalpy Flow Environments. *Aerospace* **2025**, *12*, 281. https://doi.org/10.3390/aerospace12040281



## 1. Introduction

Carbon fiber-reinforced plastic (CFRP) has the greatest specific strength and specific elasticity among all materials and is therefore widely used as the main structure of aircraft, rockets, and satellites. An example is the Ten-Koh 2 (referred to below as TK2), a low earth orbit environmental observation satellite developed by the Okuyama Laboratory of Nihon University [1]. Figure 1 shows the TK2 separated from the HTV-X and the appearance of the TK2 flight model [2]. JAXA is developing a new type of the HTV-X, which will be launched by Japan's new H3 launch vehicle [2]. The HTV-X is the successor to the HTV and is designed to

demonstrate various technologies in orbit, in addition to cargo resupply to the ISS. The first HTV-X with a cube-satellite release mission is the TK2 [2].

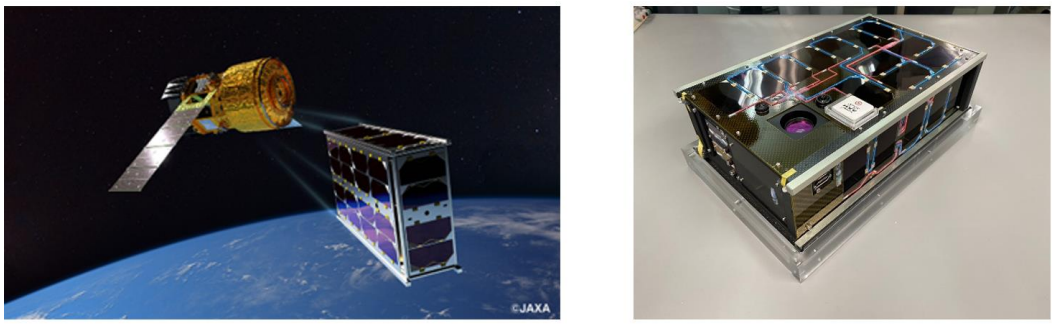


(**a**) (**b**)

**Figure 1.** (**a**) The Ten-Koh 2 separated from the first HTV-X (©JAXA); (**b**) the appearance of the Ten-Koh 2 flight model.

The TK2 is a wide 6 U (366 mm × 226 mm × 100 mm) CubeSat with a mass of about 6.8 kg, and various missions are planned in orbit. The main mission of the TK2 is a material degradation observation mission of advanced composite materials in low earth orbit (we call this a material mission), and test specimens of PEEK (poly ether ether ketone) and CF/PEEK, which are also molded by a 3D printer, and are mounted on the TK2. The test specimens will be evaluated in detail for their resistance to the space environment [3]. Nishihara et al. conducted space experiments on the ground prior to the TK2 mission and found that PEEK molded by a 3D printer degrades rapidly when exposed to short-wavelength ultraviolet (UVC) light [4]. Structural design requirements for satellites such as the TK2 generally include strength and rigidity requirements. Therefore, Okuyama et al. designed a rigid structure with a high natural frequency by combining the monocoque structure made of aluminum alloy (A7075), which is the main structure, with CFRP-laminated outer panels on all six sides of the TK2 [3]. As described above, CFRP has recently been frequently used for aerospace vehicles that require high specific strength and specific stiffness.

However, CFRP faces several technical issues. For example, CFRP is considered to have limitations in its application in future aerospace vehicles because "the matrix resin used as a material must be cryopreserved" [5], "molding takes a great deal of time, several hours" [6], "molding requires large equipment such as autoclaves" [7], and "recycling is difficult". Therefore, carbon fiber-reinforced thermoplastic composites (CFRTPs), in which carbon fibers are reinforced with thermoplastic resins such as PEEK resin, can be considered a material that can improve these problems. CFRTP has mechanical properties equivalent to those of CFRP and is suitable for injection molding and short-time press molding because it softens when the temperature is raised and hardens when the temperature is lowered, making it a material with extremely high-cost performance in mass production [8]. Other advantages of CFRTP include the ability to store the matrix resin at room temperature, a short molding time of only a few minutes, recyclability, and the ability to be molded using a 3D printer, making it a promising material for the main structure of future aircraft and spacecraft.

The sample return mission that Japan (JAXA) successfully carried out with the asteroid probe Hayabusa has been continued with Hayabusa 2 and MMX, and the sample return capsule (SRC) was made larger to accommodate the increased payload [9]. In these advanced missions, the SRC is expected to meet mission requirements such as "returning from farther away in space", "storing in a lower temperature environment", and "returning more samples". However, when responding to the requirement of "returning from

farther away in space", the SRC will be exposed to a more severe thermal environment due to the increased velocity of entry, as it is known that the heat flux due to convective heat transfer is proportional to the cube of the velocity of entry, and the heat flux due to radiative heat transfer is proportional to the 8.5th power of the velocity of entry [10]. In order to meet the requirements of "bringing back more samples" and "storing in a lower temperature environment", it is desirable to make the ablative shield covering the SRC as thin as possible to reduce the proportion of the TPS in the total weight of the SRC, and to make the ablative shield a lightweight heat shield with high heat resistance. For example, in 2010, the asteroid probe Hayabusa collected samples from the asteroid Itokawa, withstood an entry velocity of 10.61 km/s and a maximum aerodynamic heating rate of approximately 13.14 MW/m$^2$, and returned safely to Earth. The ablative material used in the SRC of Hayabusa was made of carbon Phenol and had a density of approximately 1400 kg/m$^3$, and the mass ratio of the TPS to the total weight of the SRC was over 43% [11]. For this reason, in recent years, there has been increased development of lightweight, heat-resistant ablative materials like PICA in order to increase the possible amount of onboard equipment and the payload.

The ablation cooling method is a TPS (thermal protection system) used in the most severe high-temperature environments. During atmospheric re-entry, the atmosphere in front of the re-entry capsule is compressed and the kinetic energy of the atmosphere is converted into thermal energy. The temperature rise due to this thermal energy is called aerodynamic heating, and the temperature of the atmosphere in front of the capsule exceeds 10,000 °C [12]. Figure 2 shows a conceptual diagram of ablation cooling.

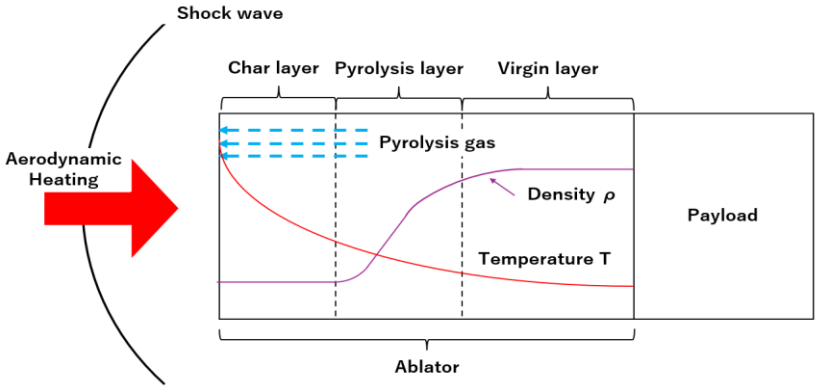


**Figure 2.** The principal of ablation.

A porous carbonized layer is formed on the surface of the ablator exposed to the intense high-temperature environment due to pyrolysis reactions. Pyrolysis gases generated during the formation of the carbonized layer pass through the carbonized layer on the porous surface to the outside of the material, forming a heat shield layer between the ablator and the atmosphere to prevent heat input from high-temperature gases. Since the pyrolysis reaction is an endothermic reaction, it also has the effect of reducing the temperature rise inside the material. Furthermore, phase transitions such as coking and sublimation also contribute to a reduction in heat conduction. Due to these cooling effects, even if the ablator surface reaches a temperature of about 3000 °C, the temperature on the back surface is suppressed to a few tens of degrees Celsius [12]. During these thermal protection processes, the ablator surface recedes due to chemical disappearances such as oxidation and sublimation, and physical disappearances such as erosion caused by aerodynamic loading and spallation caused by pyrolysis gases [13].

Because of the principle of ablation cooling as described above, ablators cannot be reused, and because the base materials of all ablators applied to recent re-entry vehicles

are thermosetting materials, repair work is very difficult if they are damaged for some reason; especially, repair work in space is almost impossible with current technology. If additional heat shields can be fabricated in a few minutes after the transportation of supplies to the Moon or Mars, and then back to the Earth, it will be possible to return to space in a short period of time. In other words, even if a heat shield is damaged during space flight, CFRTPs can be easily repaired by various fusion bonding methods due to their thermoplasticity and can be used as repair materials for heat shields since the material can be stored at room temperature for a long time.

Okuyama et al. obtained thermochemical recession characteristics of CF/Phenol through heating tests in a high enthalpy flow environment using an arc-heated wind tunnel installed at the Institute of Space and Astronautical Science (ISAS) at JAXA [14–16]. It is usually known that when an ablator made of phenolic resin is heated in a high enthalpy flow environment, the ablator surface recedes due to chemical disappearances such as oxidation and sublimation, erosion caused by aerodynamic loading, and physical disappearances such as spallation caused by pyrolysis gas [14–16]. However, Farhan et al. confirmed that 3D-printed CF/PEEK expanded in heating tests conducted at the ISAS/JAXA with heating rates of 5.0 and 14.2 MW/m$^2$ [17]. The side views of the 3D-printed CF/PEEK before and after the heat test are shown in Figure 3 [17]. As shown in Figure 3b, the side view of the 3D-printed CF/PEEK after the arc heating test shows that the interlaminar layers have peeled off and expanded slightly on the heated side. If the ablator expands, it may lead to the destruction of the heat shield due to the change in the capsule shape and aerodynamic characteristics during the re-entry flight. Therefore, this study aims to clarify the mechanism of the expansion phenomenon of CF/PEEK during heat tests and to develop a new CF/PEEK ablator that can suppress the expansion based on the mechanism.

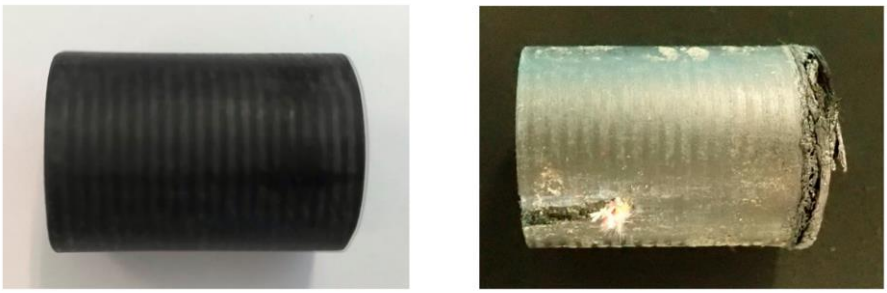


**Figure 3.** The side views of the 3D-printed CF/PEEK used in arc heating test: (**a**) a base sample before the test; (**b**) a base sample after the test [17].

## 2. Materials and Methods

### *2.1. Description of the Lightweight Ablator Series for Transfer Vehicle Systems (LATS)*

NASA previously developed a lightweight CFRP known as the phenolic-impregnated carbon ablator (PICA) [18,19]. A PICA with a density of 270 kg/m$^3$ was used as the heat shield material for the Stardust spacecraft [20,21], which collected a sample from the Wild-2 comet. Although this spacecraft was exposed to approximately 8.5 MW/m$^2$ of severe heat flux, the spacecraft successfully returned to Earth [20,21]. The lightweight PICA functioned perfectly as the heat shield material.

Recently, Okuyama et al. developed a new lightweight CFRP called the lightweight ablator series for transfer vehicle systems (LATS) [22–27] which is made from a carbon fiber felt and resin with a manufacturing method different from that of the PICA. The density of the LATS ranges between approximately 200 and 1500 kg/m$^3$; such LATS materials are exposed

to heat fluxes of approximately 200 kW/m$^2$ to 11 MW/m$^2$. Data on the thermal behaviors and performance of LATS were obtained by carrying out heating tests. From the results of these tests, the LATS was considered to function as a heat shield material in a severe environment of high enthalpy flow. This paper describes the thermal response and ablation characteristics of the LATS under such an environment. The LATS is fabricated by heating and pressurizing a material in which resin is impregnated in the carbon fiber felt. The virgin carbon felt is a polyacrylonitrile (PAN), pitch, or rayon fiber whose dried bulk density is approximately 20–1000 kg/m$^3$. The resin is mainly a Phenol or silicone resin. The LATS used for the present study was composed of a PAN carbon fiber felt with a bulk density of approximately 100 kg/m$^3$ and a Phenol resin. Heating and pressurizing are mainly carried out using the hot plate press method or the autoclave manufacturing method. The bulk density of the LATS can be adjusted by varying the quantity of resin impregnated into the felt and the pressure force of the hot plate press [22].

There are many lightweight ablators made of fiber-reinforced plastic with porous structures, such as AVCOAT used for the Apollo program and the Orion spacecraft of Artemis I, SLA series for the Mars Pathfinder program, AQ60 for the Huygens program, the PICA for the Stardust program, etc. The PICA has been improved in various ways and is now used in the OSIRIS-REX, whose main mission is to return samples from the asteroid Bennu, and in the TPS of SpaceX's Dragon spacecraft as PICA-X. The PICA is formed by the technology of impregnating Phenol resin to make a single thick sheet of carbon. On the other hand, the LATS is an accumulation of thin carbon felts impregnated with resin; the manufacturing technologies of the PICA and LATS are different [11,28].

However, although these ablators are lightweight and have high heat resistance, the matrix resins are all thermosetting resins, and as mentioned above, it is very difficult to repair them if they are damaged for some reason. An ablator using PEEK resin as the base material is considered to solve this problem. However, the thermal resistance and thermochemical recession characteristics of lightweight ablators using PEEK resin as the base material in high enthalpy flow environments have not been clarified. Therefore, in this study, we developed a LATS-type lightweight ablator (hereinafter referred to as "LATS/PEEK") using PEEK resin, which is a representative thermoplastic resin among thermoplastics, and summarized its thermal resistance and thermochemical recession characteristics in high-enthalpy flow environments. The results were compared with those of a LATS-type lightweight ablator (LATS/Phenol) made of Phenol resin, and various heating tests were conducted to experimentally examine whether LATS/Phenol can be applied as a thermal protection material in the future.

The LATS is classified into two types according to its internal structure: two-dimensional structures in which carbon felt and phenolic resin are laminated and molded in sequentially (referred to as "2DLATS") and three-dimensional structures in which carbon felt and phenolic resin are randomly mixed and molded (referred to as "3DLATS"). The differences and features between 2DLATS and 3DLATS are shown in Figure 4. As shown in Figure 4, since 2DLATS is made by laminating carbon felt and phenolic resin, pyrolysis occurs sequentially from the heated surface. On the other hand, since 3D LATS is molded by mixing rectangular carbon felt and phenolic resin, heat is transferred three-dimensionally when 3DLATS is heated, and pyrolysis gases are generated inside 3DLATS, which easily release gases on the heated surface due to its three-dimensional structure. Therefore, the arc-heating wind tunnel tests showed that although 3DLATS is more prone to mass loss than 2DLATS, the ablation cooling is larger and the internal temperature can be reduced.

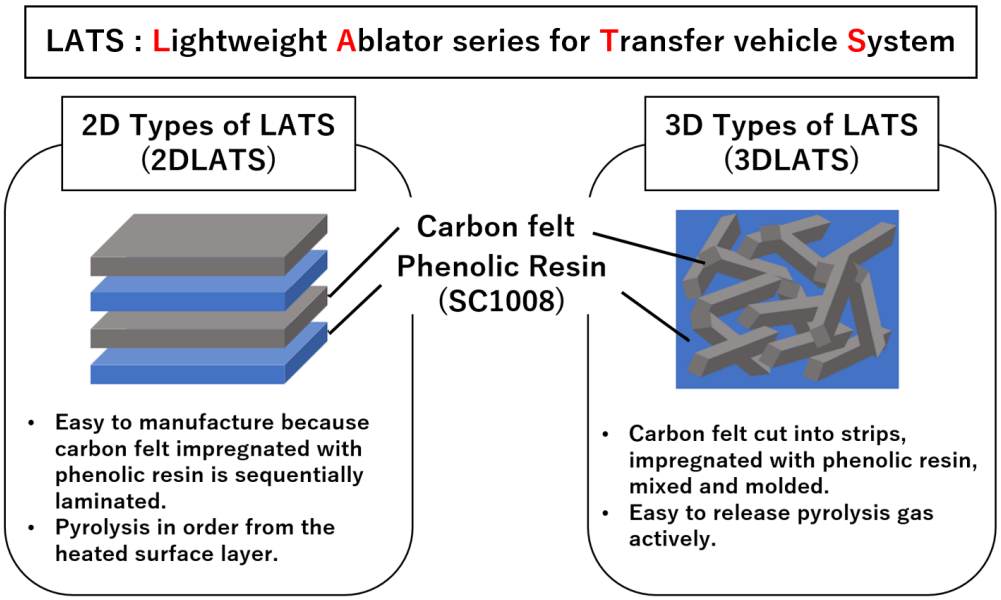


**Figure 4.** Features of different types of LATS by stacking structures.

### *2.2. Thermal Conductivity Measurement of LATS/PEEK*

To analyze the thermal response of LATS/PEEK, the thermal conductivities of 2DLATS/PEEK and 3DLATS/PEEK with different densities were measured using a steady-state thermal conductivity measurement system (TA Instruments (New Castle, DE, USA), DTC-300). DTC-300 is a device that can measure the thermal conductivity of low-to-medium-thermal-conductivity materials. The specimens were cylindrical specimens with a diameter of 50 mm and a thickness of 14~18 mm, and the measurements were performed in air. The evaluated temperature is the average temperature of the top and bottom surfaces of the specimen. The thermal conductivity measurements in this study were made at three points: 50, 100, and 250 °C.

### *2.3. Thermal Weight Loss and Thermal Expansion Behavior of LATS/PEEK*

In order to understand the expansion behavior of 2DLATS/PEEK in the lamination direction, measurements were made using thermo-mechanical analysis (TMA). TMA is a measurement method that detects the amount of deformation, such as expansion and contraction, while heating a sample under a constant static load. A Φ5 × 10 mm specimen was cut from a 2DLATS/PEEK base material with a longitudinal lamination direction. The coefficient of thermal expansion was measured through the process of increasing the temperature from room temperature to 550 °C at a rate of 5 °C/min in a nitrogen gas atmosphere using a thermo-mechanical analyzer TMA/SS-6000 manufactured by Seiko Instruments Inc. (Chiba, Japan).

Next, Φ5 × 3 mm specimens were cut from the base material of 3DLATS/PEEK in order to understand the weight loss characteristics of LATS/PEEK during the temperature increase process. Simultaneous thermo-gravimetric analysis (TGA) measurements were performed using NEXTA STA200RV, a high-performance thermal analyzer manufactured by Hitachi High-Technologies Corporation (Ibaraki, Japan), when the temperature was increased from room temperature to 1000 °C at a rate of 10 °C/min.

### *2.4. Deformation Behavior of LATS/PEEK in Arc-Heated Wind Tunnel Test*

The evaluation of thermal resistance of ablation materials in the design of an SRC is performed by a combination of thermal resistance tests in a high velocity air flow and high temperature environment using an arc-heated wind tunnel and numerical analysis of heat

conduction and surface wear and tear [22,29–31]. In the arc-heated wind tunnel, the high-temperature plasma obtained by arc discharge is expanded by a nozzle to form the test air flow, and the working gas, such as air, can be brought to a high-enthalpy state [32]. It consists of an arc heater to heat the working gas, a pressurizer and nozzle to accelerate the high-enthalpy gas at high speed, a specimen drive system, and an airflow exhaust system. The JAXA/ISAS arc heating wind tunnel tester used in this study adjusted the heating rate according to the distance from the nozzle to the specimen and could generate a maximum heating rate of 15 MW/m$^2$ when the distance from the nozzle to the specimen surface was 20 mm [32]. Figure 5 shows the appearance of the arc heating wind tunnel apparatus owned by JAXA/ISAS.

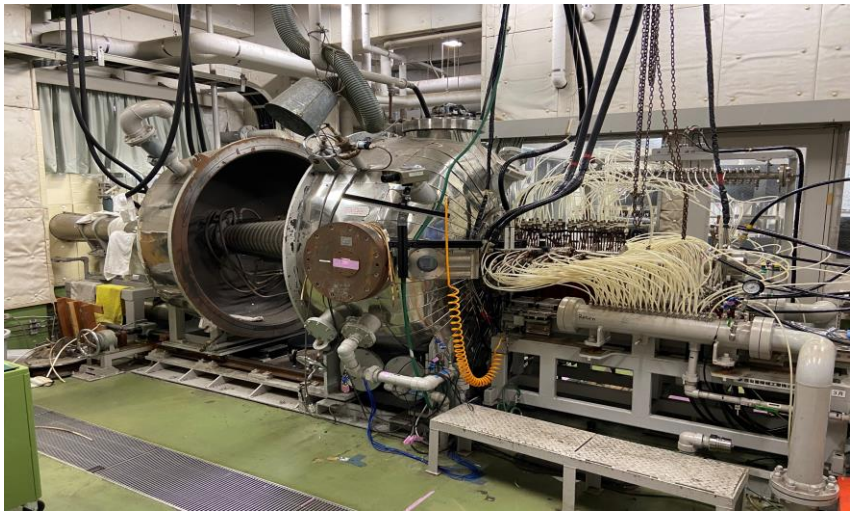

**Figure 5.** Arc heating wind tunnel facility in JAXA/ISAS.

In this study, thermo-chemical and thermal properties of various ablation materials were obtained from their surface abrasion, surface temperature, and internal temperature histories, and the applicability of these ablation materials as thermal protection materials during atmospheric re-entry was evaluated without any problem. The specimens and test conditions are shown in Table 1. Four types of specimens, Types A~D, were prepared, and the details are shown below:

1. Type A: 3D LATS/PEEK (density of 300–400 kg/m$^3$)
2. Type B: 3D LATS/PEEK (density of 500–600 kg/m$^3$)
3. Type C: 3D LATS/PEEK (density of 600–900 kg/m$^3$)
4. Type D: 3D LATS/Phenol (density of 800–900 kg/m$^3$)

Types A~C are composed of 3DLATS/PEEK, with PEEK as the matrix resin with different densities, and Type D is composed of 3DLATS/Phenol with Phenol as the matrix resin. The models of the specimens are shown in Figures 6 and 7. These specimens consisted of an evaluation ablator, which was directly heated from the front, and a support structure, which supported the ablator and suppressed the internal penetration of the side heating. The support structure was made of Bakelite, which has excellent thermal insulation performance, and the Bakelite was wrapped with glass cloth and aluminum tape. K-type thermocouples were placed inside each specimen (10, 15, and 20 mm from the front) to measure the internal temperature. During the test, the surface temperature of the heated surface was measured using a monochromatic radiation thermometer. The stagnation point pressure on the surface of the test piece shown in Table 1 was measured using a pitot pressure probe. The heating rate shown in Table 1 was measured using a gardon gauge.

**Table 1.** Specimen specifications and test conditions for heating tests at ISAS.

| Type | Specimens | | | Conditions | | | |
|---|---|---|---|---|---|---|---|
| | No. | Material | Density kg/m³ | Time [s] | Distance from Nozzle [mm] | Stagnation Pressure [kPa] | Heat Flux [MW/m²] |
| A | A-1 | 3DLATS/PEEK | 332 | 20 | 75 | 27.2 | 8.24 |
| | A-2 | | 326 | 20 | 100 | 14.8 | 4.85 |
| | A-3 | | 352 | 20 | 150 | 6.30 | 1.99 |
| B | B-1 | 3DLATS/PEEK | 549 | 20 | 50 | 49.5 | 12.6 |
| | B-2 | | 542 | 20 | 75 | 27.2 | 8.24 |
| | B-3 | | 577 | 20 | 100 | 14.8 | 4.85 |
| | B-4 | | 592 | 20 | 150 | 6.30 | 1.99 |
| C | C-1 | 3DLATS/PEEK | 894 | 20 | 50 | 49.5 | 12.6 |
| | C-2 | | 674 | 20 | 75 | 27.2 | 8.24 |
| | C-3 | | 781 | 20 | 100 | 14.8 | 4.85 |
| | C-4 | | 727 | 20 | 150 | 6.30 | 1.99 |
| D | D-1 | 3DLATS/Phenol | 865 | 20 | 150 | 6.62 | 1.88 |
| | D-2 | | 843 | 20 | 100 | 16.9 | 4.78 |
| | D-3 | | 821 | 20 | 75 | 26.9 | 8.71 |

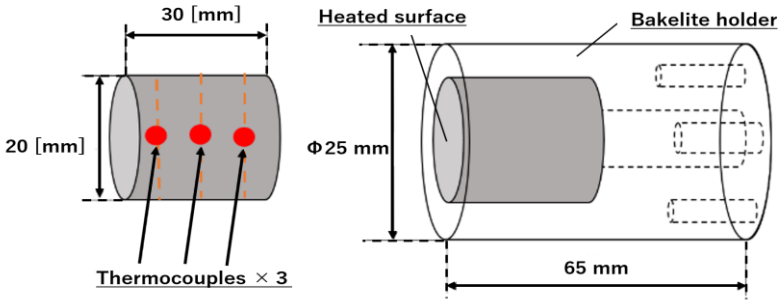


**Figure 6.** Model of specimens.


**Figure 7.** The completed sample wrapped in glass cloth and Bakelite attached to the sample holder: (**a**) the front view of the sample; and (**b**) the side view of the sample attached to the sample holder.

## 3. Results

### *3.1. Thermal Conductivity Measurement of LATS/PEEK*

The measured thermal conductivity of 2DLATS/PEEK and 3DLATS/PEEK are shown in Figure 8. Based on the obtained thermal conductivity data, a regression analysis was conducted by using the following linear function of temperature [26]:

$$\kappa = AT + B \quad (1)$$

The curve fit parameters used in Equation (1) are summarized in Table 2. The thermal conductivity of PICA with a density of 300 kg/m$^3$ is also shown in Figure 8 for reference.

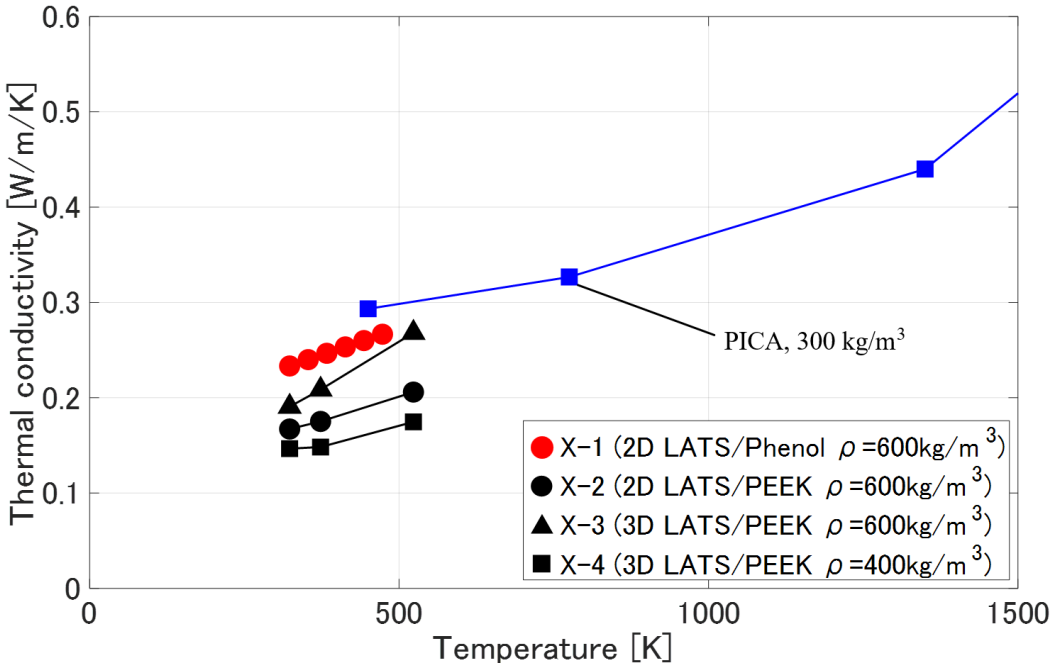


**Figure 8.** Thermal conductivity values obtained for LATS/Phenol and LATS/PEEK [19,26].

**Table 2.** Curve fit parameters in Equation (2) for thermal conductivity.

| Type | Material | Density [kg/m$^3$] | A | B |
|---|---|---|---|---|
| X-1 | 2DLATS/Phenol [26] | 600 | $2.57 \times 10^{-4}$ | $1.19 \times 10^{-1}$ |
| X-2 | 2DLATS/PEEK | 600 | $1.96 \times 10^{-4}$ | $1.57 \times 10^{-1}$ |
| X-3 | 3DLATS/PEEK | 600 | $3.90 \times 10^{-4}$ | $1.70 \times 10^{-1}$ |
| X-4 | 3DLATS/PEEK | 400 | $1.48 \times 10^{-4}$ | $1.37 \times 10^{-1}$ |

### *3.2. Thermal Weight Loss and Thermal Expansion Behavior of LATS/PEEK*

The results of the TMA measurement of 2DLATS/PEEK are shown in Figure 9. TMA is a measurement method that detects the amount of deformation, such as expansion and contraction, while heating the sample under a static constant load. The horizontal axis in Figure 9 is time [min], the left vertical axis is the amount of sample displacement TMA [mm], and the right vertical axis is the sample temperature [°C]. From Figure 10, we can see that the thermal expansion coefficient increases as the temperature approaches the melting point of the PEEK resin. Once the melting point is exceeded, the 2DLATS/PEEK softens and deforms as if being crushed. After that, it can be seen that the thermal expansion coefficient increases rapidly once the temperature exceeds 550 °C.

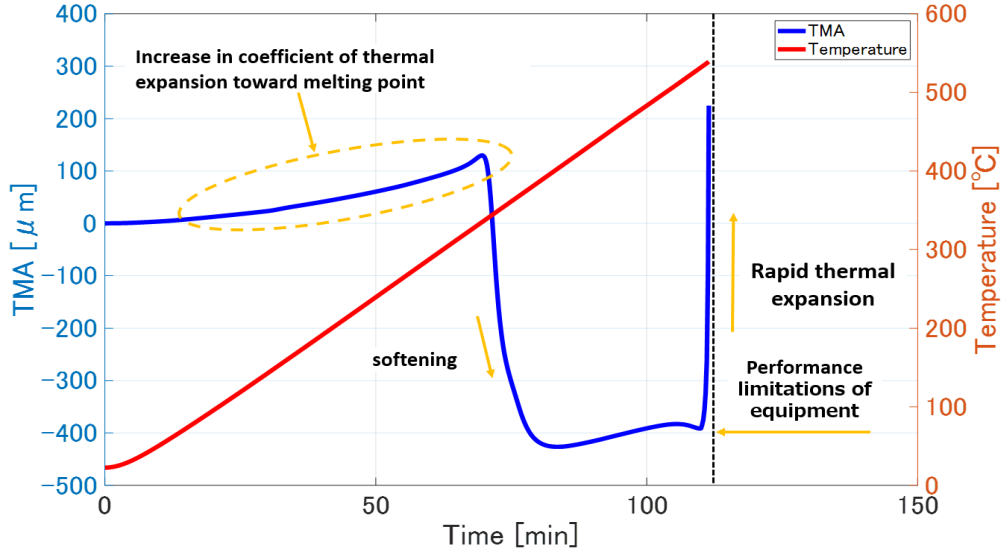


**Figure 9.** TMA histories for 2DLATS/PEEK.

The TGA measurement results for 3DLATS/PEEK are shown in Figure 10. TGA can measure the amount of weight change when a sample is heated. The horizontal axis in Figure 10 shows temperature [°C], the right vertical axis shows the percentage of mass change TG [%], and the left vertical axis shows the time derivative of TG DTG. From Figure 10, we can see that 3DLATS/PEEK begins to lose weight rapidly when the temperature exceeds about 550 °C and that thermal decomposition gas is generated.

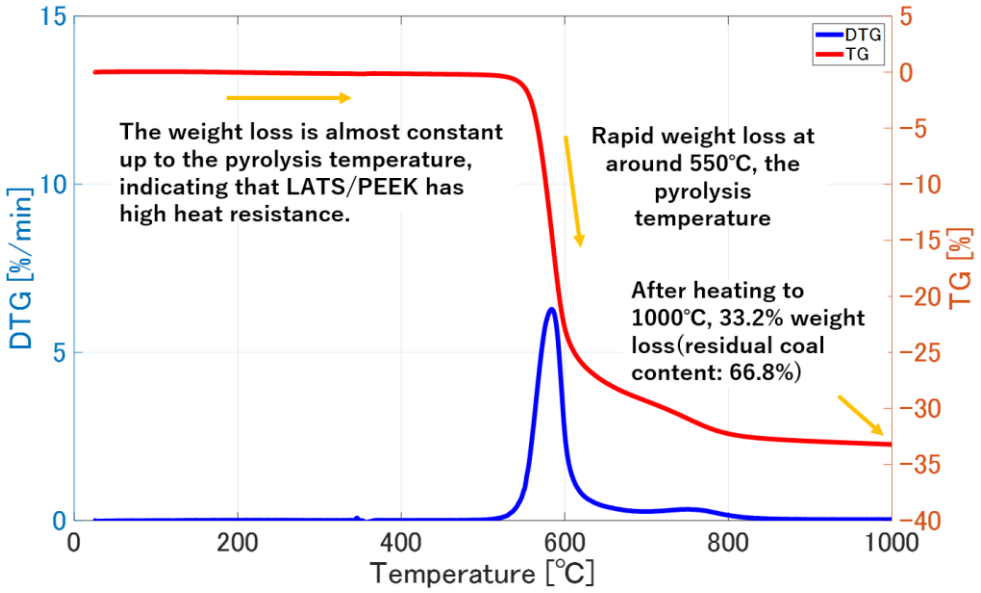


**Figure 10.** TGA histories for 3DLATS/PEEK.

### *3.3. Deformation Behavior of LATS/PEEK in Arc-Heated Wind Tunnel Test*

A side view of the arc heating test is shown in Figure 11. It is generally known that when ablation materials such as CF/Phenol are heated in a high enthalpy flow environment, such as in an arc-heated wind tunnel test, the ablator surface recedes due to chemical disappearances such as oxidation and sublimation, and also due to the thermal decomposition of the matrix resin, resulting in mass loss [14–16]. Therefore, in this study, two parameters were considered when analyzing the recession behavior of the ablator. The parameters were as follows:

1. Mass loss rate [kg/m²/s]
2. Surface recession rate [m/s]

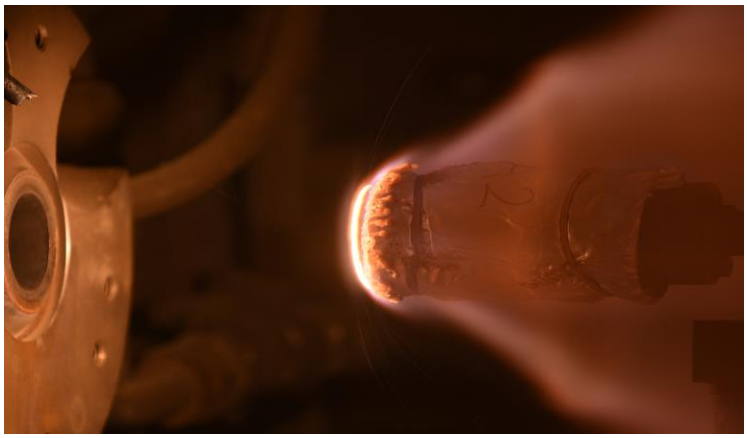

**Figure 11.** The side views of the specimen during the arc heating test.

Figure 12 shows a graph in which the horizontal axis is the maximum temperature of the specimen surface, and the vertical axis is the mass loss rate.

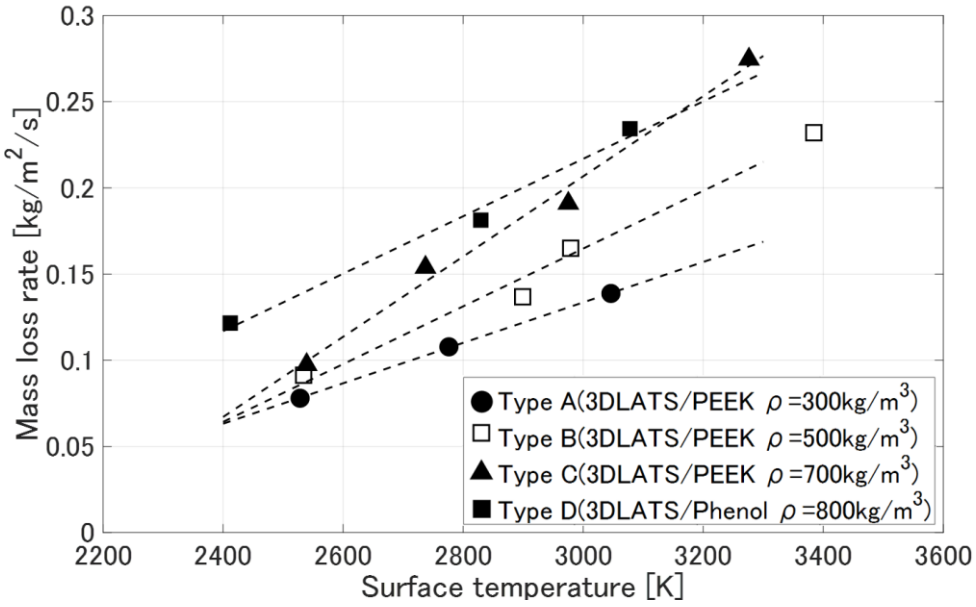


**Figure 12.** The relationship between the surface temperature and the surface mass loss rate of 3DLATS/PEEK and 3DLATS/Phenol.

Figure 13 also shows the graphs of the maximum temperature of the specimen surface on the horizontal axis and the surface recession rate on the vertical axis. The temperature of the specimen surface was measured using a radiation thermometer, and the emissivity was set to 0.85, which is a value generally used for ablation materials. Figure 13 also includes the test data of CF/PEEK made by Farhan et al. [17].

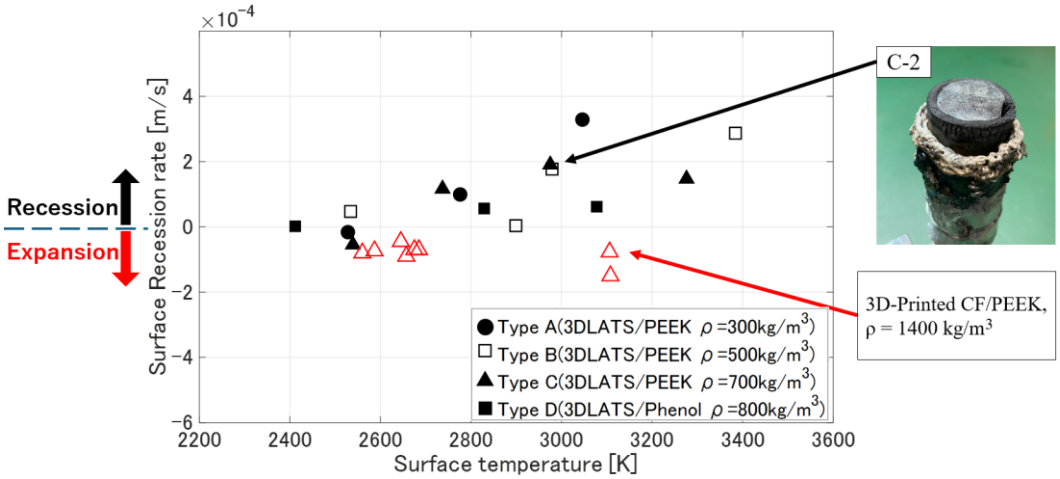


**Figure 13.** The relationship between the surface temperature and the surface recession rate of 3DLATS/PEEK and 3DLATS/Phenol.

## 4. Discussion

### *4.1. Thermal Conductivity Measurement of LATS/PEEK*

First, a comparison was made between X-1 and X-2. It can be seen that the thermal conductivity of 2DLATS/PEEK is smaller than that of 2DLATS/Phenol. Next, a comparison is made between X-2 and X-3. Figure 8 shows that the thermal conductivity of 3DLATS/PEEK is larger than that of 2DLATS/PEEK. When 2DLATS is heated, heat is conducted in the stacking order of the heated side, but when 3DLATS is heated, heat is considered to be conducted three-dimensionally due to the random arrangement of the carbon felt impregnated with the resin. In other words, it can be seen quantitatively and qualitatively that the thermal conduction properties also differ depending on the difference between the 2D and 3D lamination structures.

### *4.2. Thermal Weight Loss and Thermal Expansion Behavior of LATS/PEEK*

The TGA analysis in Figure 10 shows that the residual carbon content of LATS/PEEK when heated up to 1000 °C is 66.8%, which is almost consistent with the residual carbon content of 67% for CF/PEEK with a 30% carbon fiber content in a nitrogen atmosphere measured by Parina et al. [33] It can also be read from the DTG in Figure 10 that PEEK resin decomposes rapidly around 550 °C. On the other hand, the TGA analysis in the previous study [26] confirms that LATS/Phenol shows a gradual weight loss immediately after heating and that active pyrolysis reaction and weight loss occur after 300 °C is reached. As described above, the temperature range and amount of pyrolysis gas generated differ depending on the type of resin, and although pyrolysis reaction occurs at lower temperatures in Phenol resin compared to PEEK resin, i.e., ablation cooling can be expected from the lower temperature range, and excessive amount of pyrolysis of resin is considered to occur in order to increase the size of the SRC. Therefore, it is considered that the use of PEEK resin with a high pyrolysis temperature of 570 °C is one of the options to reduce mass loss.

Now, another issue that must be discussed here is the rapid expansion phenomenon that occurred around 550 °C in the TMA measurement of Figure 9. Many reports have been published on the expansion and deformation of ablated materials during heating tests, and Suzuki et al. discussed the deformation and degradation of materials due to pyrolysis gases and clarified that CF/Phenol expands due to very large interlayer detachment during heating tests. Suzuki et al. calculated the gas pressure inside CF/Phenol by experiments and numerical calculations and showed that the gas pressure was reduced

by setting the lamination angle [34]. Park et al. suggested that the expansion deformation increases with the increase in the carbide layer and showed that the gas pressure-induced detachment between layers occurs only in the carbide layer [35].

The expansion phenomenon of CF/Phenol when subjected to rapid heating was also reported in a previous study [36], in which the following mechanism of internal pressure increase was reported. The resin inside CF/Phenol carbonizes when heated, and gas is generated inside the material due to the vaporization of the resin during thermal decomposition. Although this gas tries to escape according to the Darcy law, if the heating is pronounced, more gas is newly released than escapes, i.e., gas pressure is generated inside the material. As a result, the gas pressure exceeds the interlayer strength of the ablator, and expansion is induced [36].

However, the mechanism by which CF/PEEK expands and deforms has not been clarified. Therefore, the authors performed TMA and TGA measurements in Figures 9 and 10, and as can be read from the results of these measurements, rapid thermal decomposition occurs around 550 °C past the TG curve, and a rapid increase in the thermal expansion coefficient is observed around 550 °C past the TMA curve, suggesting that the CF/PEEK expansion phenomenon is considered to be caused by "an increase in the pressure inside the ablator due to pyrolysis gas".

Another example is the Orion spacecraft launched by NASA as Artemis I. Artemis I was launched in November 2022 and returned safely to Earth in December of the same year. However, an examination of the heat shield of the returned Orion spacecraft revealed an unexpected loss of char. NASA engineers concluded that during the Orion spacecraft's atmospheric re-entry, the pyrolysis gas generated from the ablator, AVCOAT, used as the heat shield, failed to be released as expected, causing the internal pressure to rise and cracks to form in several carbonized locations [37]. Subsequently, repeated additional ground tests by NASA engineers and arc-heated wind tunnel tests, simulating the actual flight environment, confirmed that a "permeable" AVCOAT can successfully release the generated pyrolysis gases without cracking or delamination [37].

As described above, one of the causes of the expansion phenomenon of ablation materials exposed to high enthalpy flow is the "increase in pressure inside the ablator due to pyrolysis gas", and the development of ablation materials that avoid this phenomenon is one of the most important issues to be addressed. Various countermeasures have been taken against this problem in ablation materials used for re-entry flight vehicles. In this study, based on the expansion mechanism described above, we adopted a stacked ablator structure and a 3D structure that actively release pyrolysis gas generated when the ablator is heated to the surface of the material. Specifically, the ablators (3DLATS/PEEK), which were molded by mixing rectangularly cut carbon felt and PEEK resin as a base material, were subjected to arc-heating wind tunnel tests, which are described in the next chapter.

### *4.3. Deformation Behavior of LATS/PEEK in Arc-Heated Wind Tunnel Test*

Figure 13 shows that the surface loss rate of all the 3Dprinted CF/PEEK specimens, Type A and Type C, at the lowest heating rate (1.99 MW/m$^2$), which is negative. The surface loss value was derived from the difference between the total length of the specimens before and after the test, and the surface loss rate is expressed in unit time. Therefore, it can be seen that the surface of these specimens extends in the frontal direction, i.e., there are specimens that have expanded. Thermoplastic resins such as PEEK resin are known to rapidly increase their coefficient of thermal expansion near the glass transition temperature, the expansion phenomenon in the arc-heating wind tunnel test was caused by "an increase in pressure inside the ablator due to pyrolysis gas generated during the heating test", and the laminated structure of CF/PEEK peeled off, causing the ablator to deform in such a way that it swelled toward the surface.

On the other hand, for Types A and C (3D LATS/PEEK), expansion was slightly observed at the lowest heating rate (1.99 MW/m$^2$), but no expansion phenomenon was observed at other heating rates. This indicates that 3DLATS/PEEK is able to suppress pressure retention during the heating test, actively release pyrolysis gas, and suppress expansion deformation compared to 3D printer-made CF/PEEK. In other words, by changing the lamination structure of the ablator, it can be said that the lightweight ablator made of PEEK resin actively releases pyrolysis gases during the heating test under high enthalpy flow conditions, and ablation is successfully performed without pressure buildup inside the ablator. Figure 13 also shows that the 3DLATS/PEEK material shows a tendency toward loss under high heating rates and a tendency toward expansion under low heating rates. The reason for this deformation behavior of 3DLATS/PEEK is considered to be the effect of pressure balance on the specimen surface in addition to chemical loss, such as oxidation. Since the heating rate and stagnation pressure can be changed by the distance from the nozzle to the specimen surface in the arc-heated wind tunnel, the deformation behavior of the specimen is also considered to be affected by the pressure balance between the gas pressure due to pyrolysis gas inside the ablator and the stagnation pressure due to air flow at the ablator surface during heating tests. Therefore, additional experiments should be conducted in the future to understand the deformation behavior of 3DLATS/PEEK under heating conditions lower than 1.99 MW/m$^2$.

### *4.4. Thermo-Chemical Loss Characteristics of LATS/PEEK in Arc-Heated Wind Tunnel Tests*

Metzger et al. studied the surface recession properties of graphite during heating, and Potts clarified the surface recession properties of CF/Phenol based on Metzger et al. [38,39]. According to them, the ablation process occurs in three modes. The first mode is the rate-controlled oxidation that occurs approximately below 1230 °C. The term "rate" refers to the rate of the carbon and oxygen chemical reaction. The second mode occurs between 1230 and 2730 °C and is termed diffusion-controlled oxidation. The degradation rate is limited by the oxygen diffusion rate into the surface. The third mode, occurring above approximately 2730 °C, is termed sublimation. The sublimation of carbon occurs during the third mode.

From here, we will discuss the heat resistance properties of the test specimens (Types A to D) used in this study, particularly their thermochemical recession properties, in the context of heating tests in a high enthalpy flow environment. The surface mass loss rate in the low-temperature, rate-controlled oxidation region can be expressed by Equation (2) and the activation energy can be calculated using Equation (2) [38].

$$\dot{m}_R = k_0\sqrt{X_0 P_e}\,e^{-E/RT_w} \tag{2}$$

where, $\dot{m}_R$ is the surface mass loss rate [kg/m$^2$/s], $P_e$ is the stagnation pressure of the specimen [Pa], $k_0$ is the collision frequency [kg/(sm$^2$Pa$^{0.5}$)], $X_0$ is the mole fraction of oxygen in the air (0.21), $E$ is the activation energy [J/mol], $R$ is the universal gas constant, 8.318 J/(molK), and $T_w$ is the surface temperature of the specimen [K]. Next, taking the logarithm of both sides of Equation (2) gives us Equation (3).

$$\ln(\dot{m}_R) = -\frac{E}{RT_w} + \ln\left(k_0\sqrt{X_0 P_e}\right) \tag{3}$$

Based on Equation (3), Figure 14 shows the relationship between the horizontal axis, which is the inverse of the maximum surface temperature of the test piece ($1/T_w$ in Equation (3)), and the vertical axis, which is the logarithmic surface mass loss rate (the left side of Equation (3)). Since the slope of the approximate straight line in Figure 14 is $-E/R$ in Equation (3), the activation energy can be calculated from this.

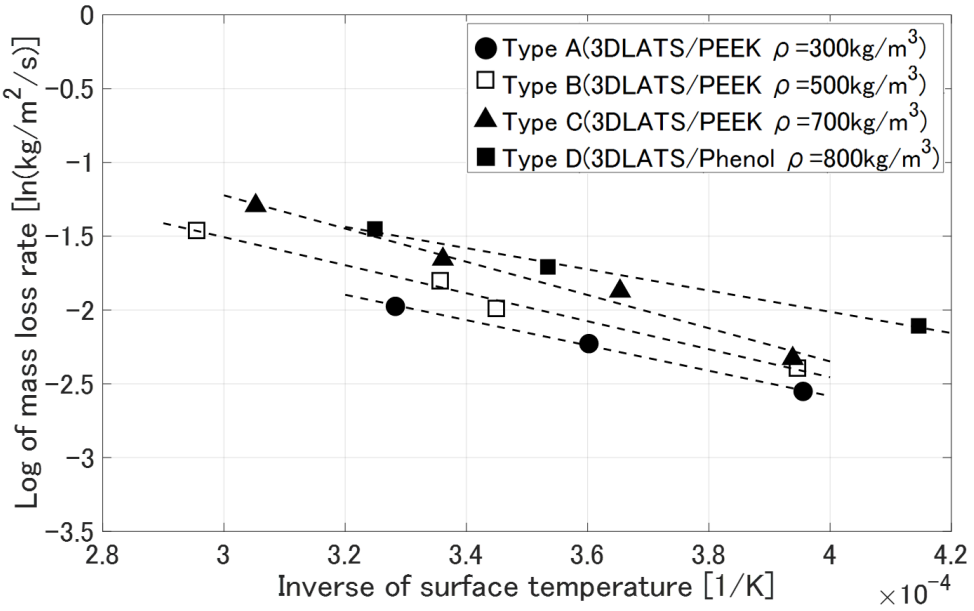


**Figure 14.** The relationship between the inverse of the surface temperature and the log of the surface mass loss rate of 3DLATS/PEEK and 3DLATS/Phenol.

The mass loss rate in the diffusion-controlled oxidation region at high temperatures can be expressed by Equation (4) using Metzger's equation [38].

$$\dot{m}_D = C_0\sqrt{P_e / R_B} \tag{4}$$

where, $\dot{m}_D$ is the surface mass loss rate [kg/m²·s], $C_0$ is the diffusion-controlled mass transfer constant [kg/m$^{3/2}$·s·Pa$^{1/2}$], and $R_B$ [m] is the blunt radius of the specimen tip. In this study, the specimen used had a flat-shaped tip, so $R_B$ was calculated as the specimen's cylindrical diameter multiplied by 2.463 (=1/0.637²). The relationship between $\sqrt{P_e / R_B}$ and the surface mass loss rate is shown in Figure 15.

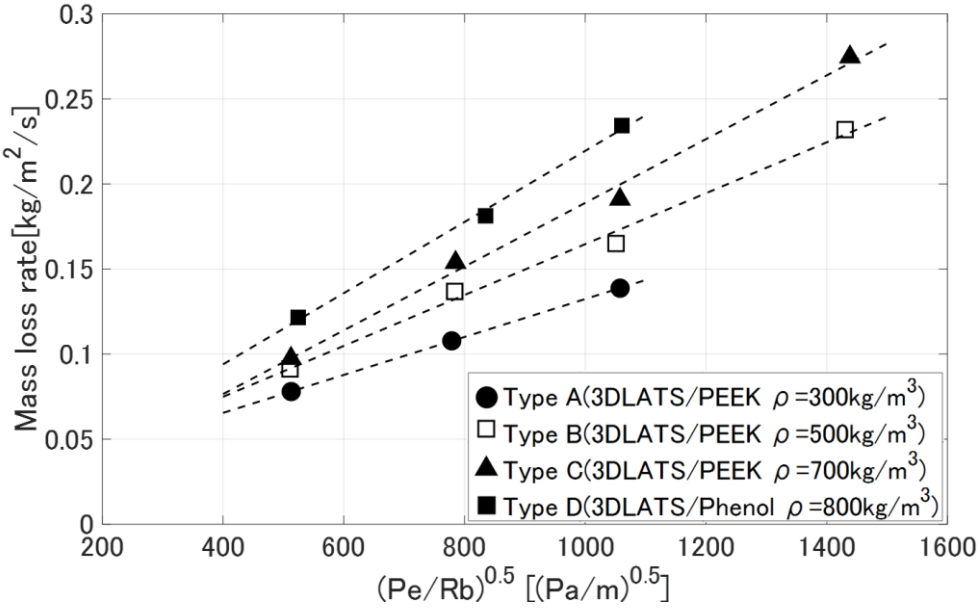


**Figure 15.** The relationship between $\sqrt{P_e / R_B}$ and the surface mass loss rate of 3DLATS/PEEK and 3DLATS/Phenol.

The two most important points in thermal protection using ablative materials are the thermal protection performance (how much can the increase in internal temperature be

lowered) and the recession properties (does it burn out before reaching the ground surface). However, if the recession of the ablative material becomes so severe that it can no longer suppress the increase in internal temperature, it will become difficult to use it as a thermal protection material, so here we will focus on recession properties and compare them. The activation energy and diffusion-controlled mass transfer constant of each ablative material are shown in Table 3.

**Table 3.** A comparison of each parameter to evaluate the thermal protection characteristics of ablators [17].

| Type | A | B | C | D | E [17] |
|---|---|---|---|---|---|
| Material | 3DLATS/PEEK | 3DLATS/PEEK | 3DLATS/PEEK | 3DLATS/Phenol | 3D-printed CF/PEEK |
| Density [kg/m$^3$] | 300–400 | 500–600 | 600–900 | 800–900 | 1400 |
| Activation Energy $E$ [kJ/mol] | 71.3 | 78.9 | 93.6 | 59.8 | 127.4 |
| Diffusion-controlled mass transfer constant $C_0$ [kg/m$^{3/2}$·s·Pa$^{1/2}$] | $1.12 \times 10^{-4}$ | $1.50 \times 10^{-4}$ | $1.87 \times 10^{-4}$ | $2.09 \times 10^{-4}$ | $2.00 \times 10^{-4}$ |

First, with regard to the activation energy E, the order was Type E > Type C > Type B > Type A > Type D, from the highest to the lowest. The activation energy E in the Arrhenius equation is the energy required for the starting material of a reaction to be excited from a low-energy state (ground state) to a high-energy state (transition state). It is also called the Arrhenius parameter, and if the activation energy barrier cannot be overcome, the reaction will not progress. Therefore, it can be seen that Type D, which has the lowest activation energy, is the most likely to undergo a reaction. This is thought to be due to the fact that the thermal decomposition temperature of phenolic resin is approximately 300 °C, which is lower than that of PEEK resin, and that ablation occurs at low temperatures. In addition, if we focus on Types A, B, and C, we can see that the activation energy decreases as the density of the test piece decreases and that the low-density LATS/PEEK is more likely to undergo ablation.

Next, the order of the diffusion-controlled mass transfer constant $C_0$ was Type D > Type E >Type C > Type B > Type A. $C_0$ is the value of the slope of the graph in Figure 15, so the larger the value, the more likely it is that mass loss will occur. In other words, it can be seen that Type D is the most likely to experience mass loss. This is thought to be due to the fact that the thermal decomposition temperature of phenolic resin is approximately 300 °C, which is lower than that of PEEK resin, and ablation occurs at low temperatures. On the other hand, if we focus on Types A, B, and C, we can see that the higher the density of the test piece, the larger the value becomes, and the high-density LATS/PEEK is more prone to mass loss.

From the above, it was clarified through the arc-heating wind tunnel test that the excessive ablation phenomenon can be suppressed because the activation energy $E$ is higher and the diffusion-controlled mass transfer constant $C_0$ of LATS/PEEK is lower than those of LATS/Phenol, respectively. These values are important parameters for designing the thickness of the ablative material, and interesting findings were obtained.

## 5. Conclusions

In order to increase the payload, a lightweight, high-heat-resistant ablative material is used in the thermal protection system (TPS) of re-entry vehicles. However, phenolic resin is often used in the ablative materials developed so far, and while they have high heat resistance, they have technical issues such as low productivity and long production

times. In this study, we developed a new ablative material (hereafter referred to as LATS/PEEK) by mixing PEEK and carbon felt. PEEK resin can be molded using various bonding methods, so it is possible to mold it together with the structure of the re-entry vehicle, and it has excellent characteristics such as a short molding time. However, in a heating test conducted in a previous study, the expansion phenomenon of CF/PEEK made with a 3D printer was confirmed [17]. If the ablative material expands, it will change the aerodynamic characteristics during re-entry flight, which is undesirable. Therefore, in this study, we aimed to elucidate the mechanism of the expansion phenomenon of the ablative material with PEEK resin as the base material and to develop a new ablative material with a laminated structure that can suppress expansion. The main conclusions are as follows:

The expansion of CF/Phenol in a rapid heating environment has been reported in previous studies [30–33], but the mechanism by which CF/PEEK causes expansion deformation has not been clarified. Therefore, the authors conducted TMA (thermo-mechanical analysis) and TGA (thermogravimetric analysis) measurements; LATS/PEEK began to lose weight rapidly after about 550 °C, and TMA shows a rapid increase in the thermal expansion coefficient at around 550 °C or higher, so it is thought that one of the causes of the expansion phenomenon of CF/PEEK is "an increase in the pressure inside the ablator due to pyrolysis gas".

In this study, based on the above expansion mechanism, arc-heating wind tunnel tests were conducted on 3DLATS/PEEK, which has a structure that allows the thermal decomposition gas generated when the ablative material is heated to be actively released on the material surface.

As a result, for types A and C (3DLATS/PEEK), although slight expansion was observed at the lowest heating rate (1.99 MW/m$^2$), no expansion was observed at other heating rates. This indicates that, compared to 3D-printed CF/PEEK, 3DLATS/PEEK is able to suppress the build-up of internal pressure during the heating test, actively release pyrolysis gas, and suppress expansion deformation. In other words, by changing the laminated structure of the ablator, we were able to demonstrate that a lightweight ablator made from PEEK resin actively releases pyrolysis gas and causes good ablation in heating tests under a high enthalpy flow environment.

In the arc-heated wind tunnel test, it was also found that 3DLATS/PEEK shifted to the recession side under high heating rate conditions and to the expansion side under low heating rate conditions. The reason for this deformation behavior of 3DLATS/PEEK is thought to be due to the pressure balance on the specimen surface in addition to chemical losses, such as oxidation. This is because the heating rate and stagnation point pressure can be changed by the distance from the nozzle to the specimen surface in the arc-heated wind tunnel, so the deformation behavior of the specimen is also thought to be affected by the pressure balance on the ablator surface between the gas pressure from the pyrolysis gas inside the ablator and the stagnation point pressure from the airflow during the heating test. Therefore, it is necessary to conduct additional experiments to understand the deformation behavior of 3DLATS/PEEK under heating conditions lower than 1.99 MW/m$^2$.

**Author Contributions:** Conceptualization, M.O., K.-i.O., S.H. and T.I.; Methodology, M.O., K.-i.O. and S.H.; Software, M.O. and K.-i.O.; Validation, M.O., K.-i.O. and S.H.; Formal analysis, M.O., K.-i.O. and S.H.; Investigation, M.O., K.-i.O. and S.H.; Resources, K.-i.O.; Data curation, M.O., S.H. and T.I.; Writing—original draft, M.O., K.-i.O. and S.H.; Writing—review & editing, K.-i.O.; Visualization, K.-i.O.; Supervision, K.-i.O.; Project administration, M.O., K.-i.O., S.H. and T.I.; Funding acquisition, K.-i.O. All authors have read and agreed to the published version of the manuscript.

**Funding:** This research received no external funding

**Data Availability Statement:** The raw data supporting the conclusions of this article will be made available by the authors on request.

**Acknowledgments:** The high enthalpy flow heating experiments were conducted at the arc wind tunnel facility provided by the Institute of Space and Astronautical Science (ISAS), Japan Aerospace Exploration Agency (JAXA) as an inter-university research institute facility (Project ID: WA24-10). We would like to express our gratitude to all those involved at the ISAS of JAXA.

**Conflicts of Interest:** The authors declare no conflicts of interest.

## References

1. Okuyama, K.; Rodriguez Leon, R.A.; Fajardo Tapia, I.; Ten-Koh 2 Team. Completion of the Development of Ten-Koh 2 Spacecraft. In Proceedings of the 33rd International Symposium on Space Technology and Science, Kurume, Japan, 6–9 June 2023.
2. Ito, N.; Sasaki, H. Development Status of New Space Station Transfer Vehicle (HTV-X), Council for Science and Technology, Research Planning and Evaluation Subcommittee, Space Development and Utilization Subcommittee. 2021. Available online: https://www.mext.go.jp/content/20210209-mxt_uchukai01-000012798_10.pdf (accessed on 25 February 2025). (In Japanese)
3. Nishihara, K.; Okuyama, K.; Rodriguez, R.; Fajardo, I. The Thermo-Mechanical Properties of Carbon-Fiber-Reinforced Polymer Composites Exposed to a Low Earth Orbit Environment. *Aerospace* **2021**, *11*, 201.
4. Okuyama, K.; Yoshikawa, K.; Oue, C. A Simple Method for Identifying the Natural Frequency of a Micro Satellite with a Primary Structure Made of Aluminum Alloy. *Aerospace* **2021**, *11*, 436.
5. Campbell, F.C. Chapter 5—Ply Collation: A Major Cost Driver. In *Manufacturing Processes for Advanced Composites*; Campbell, F.C., Ed.; Elsevier Science: Amsterdam, The Netherlands, 2004; pp. 131–173.
6. Campbell, F.C. Chapter 10—Thermoplastic Composites: An Unfulfilled Promise. In *Manufacturing Processes for Advanced Composites*; Campbell, F.C., Ed.; Elsevier Science: Amsterdam, The Netherlands, 2004; pp. 357–397.
7. Diaz, J.; Rubio, L. Developments to Manufacture Structural Aeronautical Parts in Carbon Fiber Reinforced Thermoplastic Materials. *J. Mater. Process. Technol.* **2003**, *143–144*, 342–346.
8. Matsuzaki, R. Next Generation Molding Technology: Continuous Carbon Fiber 3D Printing. In *The Future of Carbon Fibers and Carbon Fiber Composites*; Tokyo University of Science: Tokyo, Japan, 2018; Chapter 5, Section 5.2.
9. Kazuhiko, Y. Research and Development on Advanced Sample Return Capsule for Future Deep Space Exploration. In Proceedings of the 67th Space Sciences and Technology Conference, 1H11, Toyama, Japan, 17–20 October 2023.
10. Caldwell, A.; Feldman, J. Reusable TPS Past, Present, & Future, Entry Systems and Technology Division Ames Research Center, NASA, June 2023. Available online: https://ntrs.nasa.gov/api/citations/20230009259/downloads/EDL%20Seminar%20-%20Reusable%20TPS%20Past%20Present%20and%20Future%20v4.0.pdf (accessed on 5 December 2023).
11. Parcero, K.; Witkowski, A.; Davies, C. Planetary Mission Entry Vehicles, Quick Reference Guide, Ver. 4.1, SP-20230010341, NASA. Available online: https://www.nasa.gov/wp-content/uploads/2023/08/final-planetary-mission-entry-vehicles-quick-reference-guide-v4.1-.pdf (accessed on 5 December 2023).
12. Yamada, T.; Abe, T. Plasma Phenomena and Surrounding Effects During the Earth Atmospheric Reentry of the Hayabusa Capsule. *J. Plasma Fusion Res.* **2006**, *82*, 368–374.
13. Kubota, H.; Suzuki, K.; Watanuki, T. *Thermogas Dynamics of Spacecraft*; University of Tokyo Press: Tokyo, Japan, 2002; pp. 97–156.
14. Okuyama, K.; Zako, M. A Study on Recession Characteristics of Completely Carbonized CFRP. *Aerosp. Technol. Jpn.* **2004**, *3*, 35–43. (In Japanese)
15. Okuyama, K.; Kato, S.; Yamada, T.; Zako, M. Oxidation Characteristics of the Carbonized CFRP under the Air Environments. *TANSO* **2004**, *213*, 128–133. (In Japanese).
16. Okuyama, K.; Kato, S.; Yamada, T. Thermo-Chemical Recession Characteristics of CFRP in an Earth Atmospheric Re-entry Environment. *TANSO* **2005**, *219*, 232–237. (In Japanese).
17. Abdullah, F.; Okuyama, K.; Morimitsu, A.; Yamagata, N. Effects of Thermal Cycle and Ultraviolet Radiation on 3D Printed Carbon Fiber/Polyether Ether Ketone Ablator. *Aerospace* **2020**, *7*, 95. https://doi.org/10.3390/aerospace7070095.
18. Tran, H.; Johnson, C.; Rasky, D.; Hui, F.; Chen, Y.K.; Hsu, M. Phenolic Impregnated Carbon Ablators (PICA) for Discovery Missions. In Proceedings of the 31st AIAA Thermophysics Conference, New Orleans, LA, USA, 17–20 June 1996; AIAA Paper 96-1911.

19. Tran, H.; Johnson, C.; Rasky, D.; Hui, F.; Hsu, M.; Chen, T.; Chen, Y.K.; Paragas, D.; Kobayashi, L. *Phenolic Impregnated Carbon Ablators (PICA) for Discovery Missions, NASA TM 110440*; NASA: Washington, DC, USA, 1997.
20. Desai, P.N.; Mitcheltree, R.A.; Cheatwood, F.M. Entry Dispersion Analysis for the Stardust Comet Sample Return Capsule. In Proceedings of the GNC, AFM, and MST Conference and Exhibit, New Orleans, LA, USA, 11–13 August 1997; AIAA Paper 97-3812.
21. Willcockson, W.H. Stardust Sample Return Capsule Design Experience. *J. Spacecr. Rocket.* **1999**, *36*, 470–474.
22. Okuyama, K.; Kato, S.; Ohya, H. Thermochemical Performance of a Lightweight Charring Carbon Fiber Reinforced Plastic. *J. Jpn. Soc. Aeronaut. Space Sci.* **2013**, *56*, 159–169. (In Japanese).
23. Kobayashi, Y.; Sakai, T.; Okuyama, K.; Suzuki, T.; Fujita, K.; Kato, S. An Experimental Study on Thermal Response of Low Density Carbon-Phenolic Ablators. In Proceedings of the 47th AIAA Aerospace Sciences Meeting Including the New Horizons Forum and Aerospace Exposition, Orlando, FL, USA, 5–8 January 2009; AIAA Paper 2009-1587.
24. Suzuki, T.; Fujita, K.; Sakai, T.; Okuyama, K.; Kato, S.; Nishio, S. Evaluation of Prediction Accuracy of Thermal Response of Ablator under Arcjet Flow Conditions. In Proceedings of the 10th AIAA/ASME Joint Thermophysics and Heat Transfer Conference, Chicago, IL, USA, 28 June–1 July 2010; AIAA Paper 2010-4787.
25. Sakai, T.; Inoue, T.; Kuribayashi, M.; Okuyama, K.; Suzuki, T.; Fujita, K.; Kato, S.; Nishio, S. Post-Test Sample Analysis of Low Density Ablators Using Arcjet. *Trans. Jpn. Soc. Aeronaut. Space Sci. Aerosp. Technol.* **2012**, *10*, 65–71.
26. Suzuki, T.; Fujita, K.; Sakai, T.; Okuyama, K.; Kato, S.; Nishio, S. Thermal Response Analysis of Low Density CFRP Ablator. *Trans. Jpn. Soc. Aeronaut. Space Sci. Aerosp. Technol.* **2012**, *10*, 21–30.
27. Kato, S.; Okuyama, K.; Gibo, K.; Miyagi, T.; Suzuki, T.; Fujita, K.; Sakai, T.; Nishio, S.; Watanabe, A. Thermal Response Simulation of Ultra-Light Weight Phenolic Carbon Ablator by the Use of the Ablation Analysis Code. *Trans. JSASS Aerosp. Technol. Jpn.* **2012**, *10*, Pe31–Pe39.
28. Johnson, S.M. Thermal Protection Materials and Systems: Past, Present, and Future. In Proceedings of the Missouri University of Science and Technology, Rolla, MO, USA, 4 April 2013.
29. Okuyama, K.; Kato, S.; Yamada, T. *USERS REV Capsule Research, Development and a Post-Flight Analysis*; JAXA Research and Development Report; JAXA-RR-04-045; JAXA: Tokyo, Japan, 2005; pp. 55–76. (In Japanese)
30. Schneider, P.J.; Dolton, T.A.; Reed, G.W. Mechanical Erosion of Charring Ablators in Ground-Test and Re-entry Environments. *AIAA J.* **1968**, *6*, 64–72.
31. Potts, R.L. Application of Integral Methods to Ablation Charring Erosion, A Review. *J. Spacecr. Rocket.* **1995**, *32*, 200–209.
32. Shimoda, T.; Yamada, K. Status and Development of Arc Wind Tunnel in JAXA/ISAS. *Aerosp. Technol. Jpn.* **2015**, 315–320. Available online: https://www.jstage.jst.go.jp/article/kjsass/63/10/63_KJ00010078682/_pdf (accessed on 25 February 2025). (In Japanese)
33. Patel, P.; Hull, T.R.; McCade, R.W.; Flath, D.; Grasmeder, J.; Percy, M. Mechanism of Thermal Decomposition of Poly(Ether Ether Ketone)(PEEK) From a Review of Decomposition Studies. *Polym. Degrad. Stab.* **2010**, *95*, 709–718.
34. Suzuki, T.; Sawada, K.; Yamada, T.; Inatani, Y. Thermal Response of Ablative Test Piece in Arc-Heated Wind Tunnel. In Proceedings of the 42nd AIAA Aerospace Sciences Meeting, Reno, NV, USA, 5–8 January 2004; AIAA 2004-341.
35. Park, C. Stagnation-Point Ablation of Carbonaceous Flat Disks—Part II: Experiment. *AIAA J.* **1983**, *21*, 1748–1754.
36. Koyanagi, J.; Fukuda, Y.; Yoneyama, S.; Hirai, K.; Yoshimura, A.; Aoki, T.; Ogasawara, T. Local Out-of-Plane Deformation of CFRP Ablator Subjected to Rapid Heating. *J. Jpn. Soc. Compos. Mater.* **2016**, *42*, 146–152.
37. Peters, E. NASA Identifies Cause of Artemis I Orion Heat Shield Char Loss. 5 December 2024. Available online: https://www.nasa.gov/missions/artemis/nasa-identifies-cause-of-artemis-i-orion-heat-shield-char-loss/ (accessed on 5 December 2024).
38. Metzger, J.W.; Engel, M.J.; Diaconis, N.S. Oxidation and Sublimation of Graphite. *AIAA J.* **1967**, *5*, 425–431.
39. Potts, R.L. Hybrid Integral/Quasi-Steady Solution of Charring Ablation. In Proceedings of the 5th Joint Thermophysics and Heat Transfer Conference, Seattle, WA, USA, 18–20 June 1990.